

Digital radio detection of cosmic rays: achievements, status and perspectives

Tim Huege

Karlsruhe Institute of Technology, Institut für Kernphysik, Karlsruhe

Abstract. Over the past decade, radio detection of cosmic rays has matured from small-scale prototype experiments to installations spanning several km^2 with more than a hundred antennas. The physics of the radio signal is well understood and simulations and measurements are in good agreement. We have learned how to extract important cosmic ray parameters such as the geometry of the air shower and the energy of the primary particle from the radio signal, and have developed very promising approaches to also determine the mass of the primary particles. At the same time, limitations have become increasingly clear. I review the progress made in the past decade and provide a personal view on further potential for future development.

Keywords: cosmic rays, air showers, radio emission

PACS: 96.50.sd, 95.55.Jz

INTRODUCTION

A decade has passed since the field of radio detection of cosmic ray air showers has been revived by the LOPES [1] and CODALEMA [2] experiments. Since then, we have progressed from small-scale prototype installations to arrays with instrumented areas of several km^2 . A fundamental breakthrough has been achieved with a detailed understanding of the radio emission mechanisms. On the basis of this understanding, analysis procedures have been developed to extract the air shower characteristics of interest, in particular the arrival direction, primary particle energy and depth of shower maximum. In this article I will give a concise overview of the achievements of the past decade, focusing in particular on the most recent results, and then give a short outlook on the future application potential of the technique.

ACHIEVEMENTS OF THE LAST DECADE

Major milestones on the way towards a full exploitation of the radio detection technique have been reached in the past decade. The following represents an incomplete selection, focused in particular on recent results which have preferably been published in peer-reviewed journal articles.

Radio emission physics

Several approaches have been followed to achieve a detailed understanding of the physics of the radio emission from extensive air showers. It has been very fruitful to approach the problem from two perspectives: on the one hand, microscopic Monte Carlo simulations [3, 4, 5] have been developed which calculate the radio emission based on air shower simulations and classical electrodynamics without any free parameters; on the other hand, macroscopic models [6, 7], have been used to calculate the emission by superposing “emission mechanisms”. From the combination of all these works, we have learned that the radio emission can be interpreted as a superposition of geomagnetic radiation from time-varying transverse currents [8] and the Askaryan effect [9] induced by the time-varying net charge excess in the shower (Fig. 1). Both mechanisms have peculiar polarization characteristics. Their superposition leads to a pronounced asymmetry in the radio emission footprint on the ground, as shown in Fig. 2. The emission from individual electrons and positrons in the shower adds up coherently, especially at frequencies below 100 MHz. The refractive index gradient in the atmosphere leads to a relativistic time-compression of the emitted radio pulses for observers located near the Cherenkov angle, so that at these locations emission can be observed up to GHz frequencies [10].

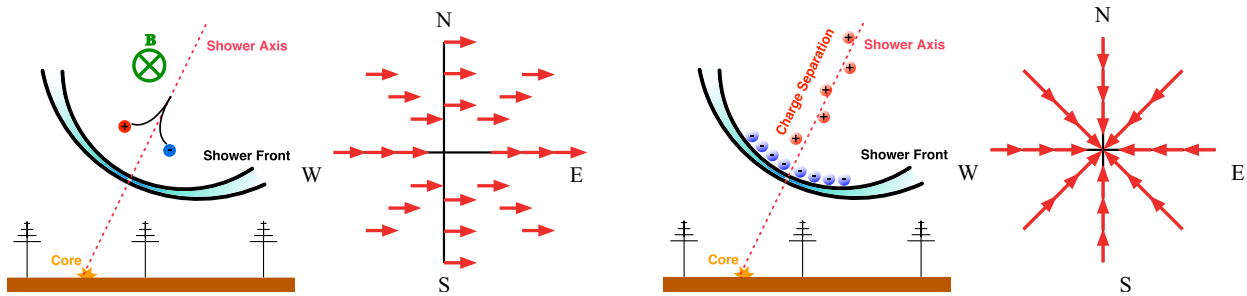


FIGURE 1. The radio emission from air showers can be interpreted as a superposition of geomagnetic (left) and charge excess (right) emission with specific polarization patterns. Diagrams are from [11] and K.D. de Vries.

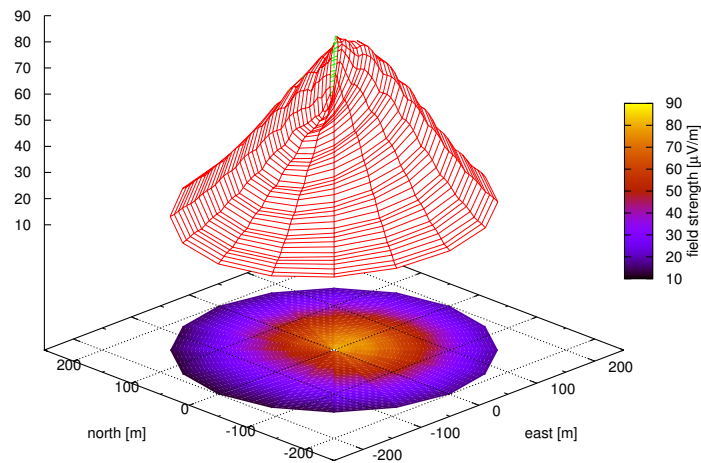


FIGURE 2. Superposition of the geomagnetic and charge excess contributions produces a pronounced asymmetry in the footprint of the radio emission, as here shown for a CoREAS simulation [3].

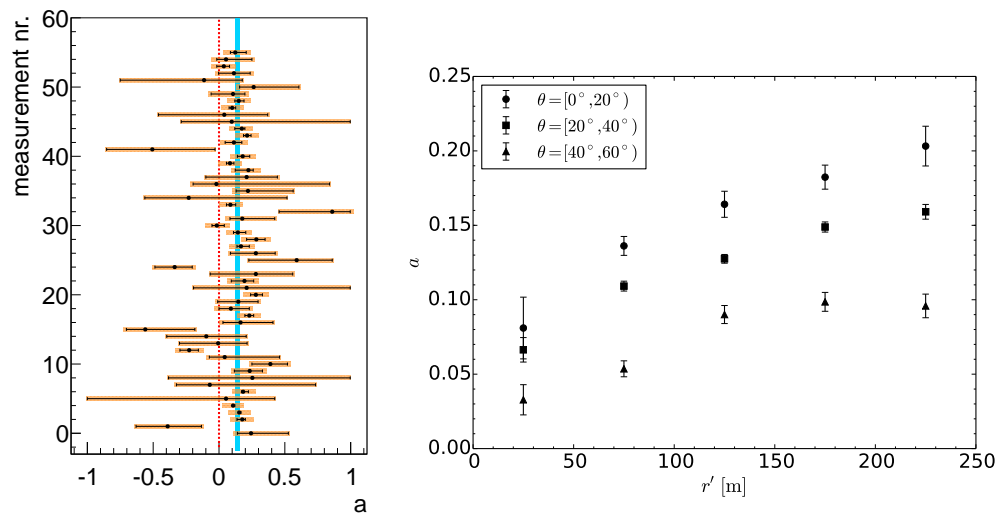


FIGURE 3. With AERA, the relative contribution of an emission component with radially aligned electric field vectors, as expected for the charge excess emission, was quantified in individual measurements (left). The average relative strength was measured to be 14% [16]. With LOFAR, it could be shown that the relative strength is a function of zenith angle and lateral distance (right) [17].

Strength of the charge excess contribution

While the geomagnetic emission mechanism has been identified already in the historical works [12], the charge excess contribution was first established by the modern experiments. An analysis of CODALEMA data first established the asymmetry of the radio footprint, a signature of the superposition of both mechanisms [13]. With AERA the first quantitative measurement of an emission contribution with radially aligned electric field vectors was made [14]. The relative strength of this emission was quantified with an average value of 14% (Fig. 3 left). With LOFAR [15] it has now been shown that this value is in fact not a constant but varies with lateral distance and zenith angle (Fig. 3 right), as is also expected from simulations. Readers should keep in mind that for different experiments with different geomagnetic field configurations, the values are expected to be different. It is important to know the strength of this relative contribution as well as possible so that it can be corrected for in analyses procedures.

Energy reconstruction

It has long been known that the radio electric field strength scales linearly with the primary particle energy, as it should for coherent radiation. Exploiting geometrical influences on the emission, the influence of shower-to-shower-fluctuations can be minimized and simulations predict an intrinsic energy resolution of radio measurements of well below 10% [18].

Many experiments have reported correlations of particle energy and radio amplitudes, but the only quantitative publication in a peer-reviewed journal so far has been made by LOPES [19]. This analysis confirmed with modern simulations that intrinsically an energy resolution of better than 10% should be achievable (Fig. 4 left). Measured LOPES data confirm the predicted linear scaling and achieve a combined energy resolution of KASCADE-Grande and LOPES of $\approx 20\%$ (Fig. 4 right). This is remarkable as the KASCADE-Grande energy resolution alone is approximately 20%. Work on energy determination by Tunka-Rex [20] and AERA is ongoing, and initial results having been shown at this conference. An interesting point will be to compare the absolute energy scales derived with the different experiments in light of the challenge of absolute calibration of the detectors.

Precise calorimetric energy measurements with radio antennas can be very valuable to cross-check the energy scales of other techniques such as surface particle detectors and fluorescence telescopes. The intrinsic high energy resolution, the sensitivity to the electromagnetic component of the air shower alone, and the fact that the radio emission can be calculated from first principles and does not suffer attenuation in the atmosphere makes this approach very promising for future studies.

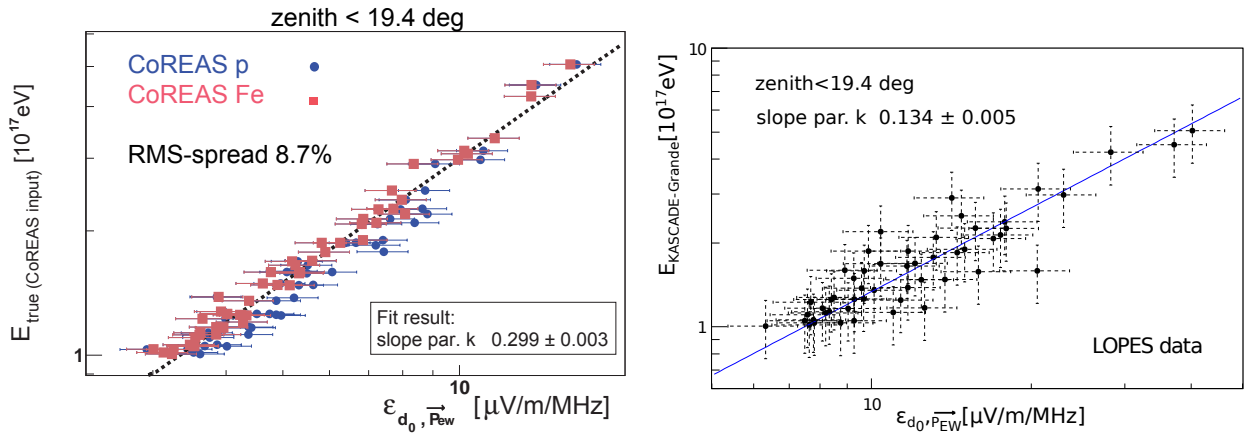


FIGURE 4. Correlation between radio amplitude and Monte Carlo true energy as predicted with CoREAS simulations for LOPES data (left) and actual linear correlation measured with LOPES (right) [19].

Xmax reconstruction

Radio emission from air showers contains information on the distance of the radio source and thus the depth of shower maximum [18], X_{\max} , the primary mass-sensitive parameter used in air shower physics. First experimental proof that the lateral distribution function of radio signals is sensitive to the shower evolution, in this case probed with muon pseudorapidities measured by KASCADE-Grande, was published by the LOPES experiment [21].

A quantitative analysis of LOPES data in direct comparison with CoREAS simulations showed that from the measured lateral slopes of the radio signals, X_{\max} values can be reconstructed which are consistent with the expectation for a mass composition between the extremes of pure proton and iron primaries (Fig. 5 left) and measurements from established experiments with X_{\max} sensitivity (Fig. 5 right). The method applied to LOPES data was kept fairly simple, as the data quality was a limiting factor and no independent reference X_{\max} information could be used for comparison. The resulting method uncertainty was 50 g cm^{-2} and the total systematic uncertainty was estimated to at most 90 g cm^{-2} , which is not competitive with measurements by established techniques such as Fluorescence detection, which reaches a resolution of 20 g cm^{-2} .

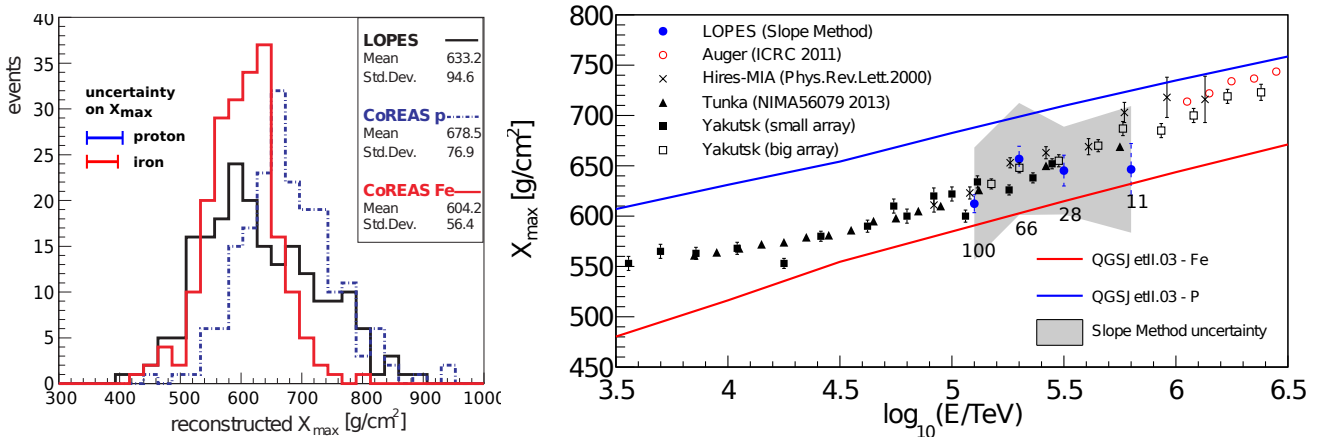


FIGURE 5. From the slope of the radio lateral distribution functions, an X_{\max} measurement for each individual showers can be derived from LOPES data in combination with CoREAS simulations (left). The resulting mean X_{\max} values as a function of energy are consistent with measurements from other experiments (right). Both results are from [19].

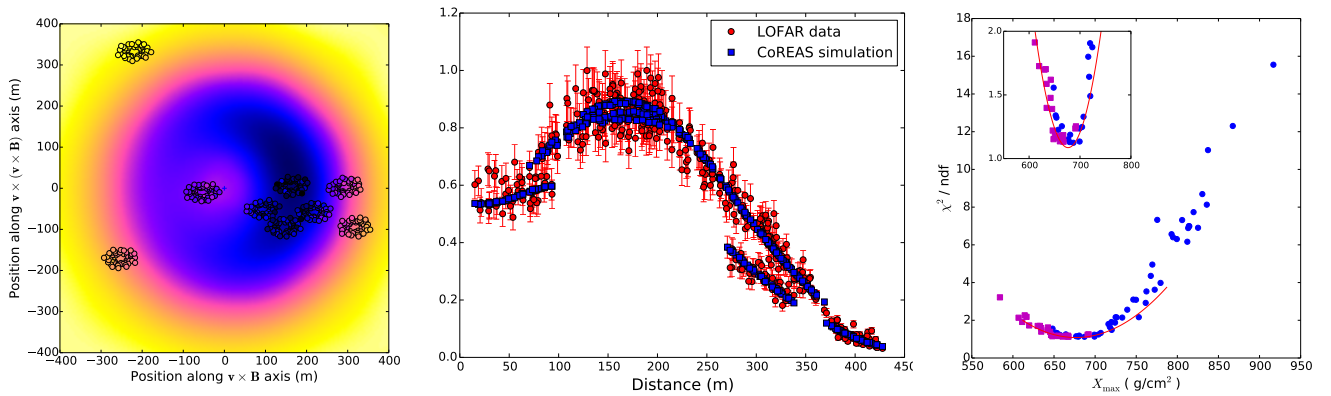


FIGURE 6. Comparison between a LOFAR measurement of an air shower (left, circles) and a CoREAS simulation (left, background color). A one-dimensional projection (middle) illustrates the impressive agreement and the pronounced structure due to Cherenkov-like time compression and asymmetries. The dominating parameter governing fit quality is X_{\max} , which can in turn be determined with high resolution from comparison with multiple simulations (right). All diagrams are from [22].

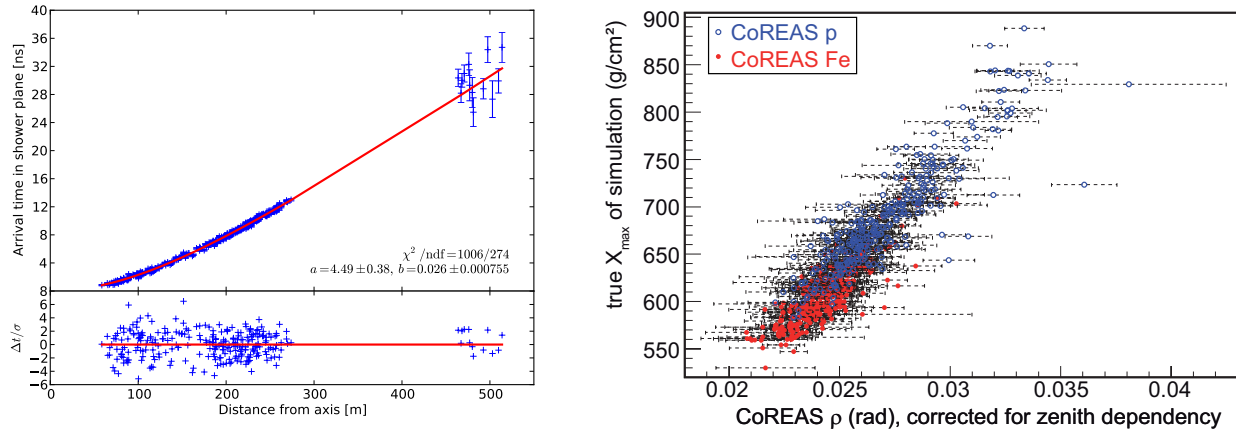


FIGURE 7. LOFAR has experimentally confirmed that the radio wavefront can be best described by a hyperbola (left) [23]. In a LOPES analysis it has been shown how the opening angle of the asymptotic cone of the hyperbola can be used to determine X_{max} (right) [24].

LOFAR has recently demonstrated, however, that if a detailed measurement of the complex two-dimensional radio footprint with all its asymmetries and structure is available, X_{max} can be determined with a resolution of less than 20 g cm^{-2} . This is done by simulating radio emission profiles and comparing them with measurements (Fig. 6 left and middle) until the best possible agreement has been found. The dominating parameter governing fit quality is the depth of shower maximum, which can in turn be read off from the comparison with simulations (Fig. 6 right).

In addition to exploiting the amplitude distribution of the radio signal, it has long been predicted that also the radio emission wavefront can be used to determine the source distance and thus X_{max} . LOPES had predicted that a hyperbolic wavefront describes the arrival times best, which has now been shown very clearly by LOFAR (Fig. 7 left). After fixing an offset parameter, the opening angle of the asymptotic cone of the hyperbola can be used to determine X_{max} directly, as has been shown in a LOPES analysis on the basis of CoREAS simulations (Fig. 7 right). The achievable precision is predicted to be approximately 30 g cm^{-2} .

Studies at AERA and Tunka-Rex, where independent X_{max} measurements are available for comparison with the radio results, will provide experimental verification of these reconstruction approaches soon. The most promising strategy will of course be to combine these two methods in a joint analysis, possibly complemented by further observables such as the pulse shape or frequency spectral index.

FUTURE POTENTIAL

Many successes have already been achieved, and with the detailed understanding of the radio emission physics, the potential for the future can be better evaluated than it could be a number of years ago. I stress that the following is my personal view, which might not be shared by everybody else.

Two complementary paths are currently being followed in the field. One is to try to cover larger and larger areas. AERA currently covers 6 km^2 with 124 detector stations. The original hope was that areas as large as the one of the Pierre Auger Observatory with its 3000 km^2 could soon be covered with radio antennas as an additional detector. It has become clear by now, however, that the radio emission footprint for air showers with zenith angles below 60° only has a size of a few hundred meters in radius (Fig. 8), independent of the primary particle energy. To be able to extract X_{max} information from radio signals alone it seems that an antenna spacing significantly larger than $\approx 300 \text{ m}$ is insufficient. This means that large areas would need instrumentation with a very high number of antennas. The current concepts are not scalable to arrays with thousands of antennas. Considerable research & development is needed if one wants to achieve this goal. Inclined air showers, however, produce very large radio footprints because the radio source moves far away (Fig. 8 right). This is not a pure projection effect and was realized early on [25]. While the X_{max}

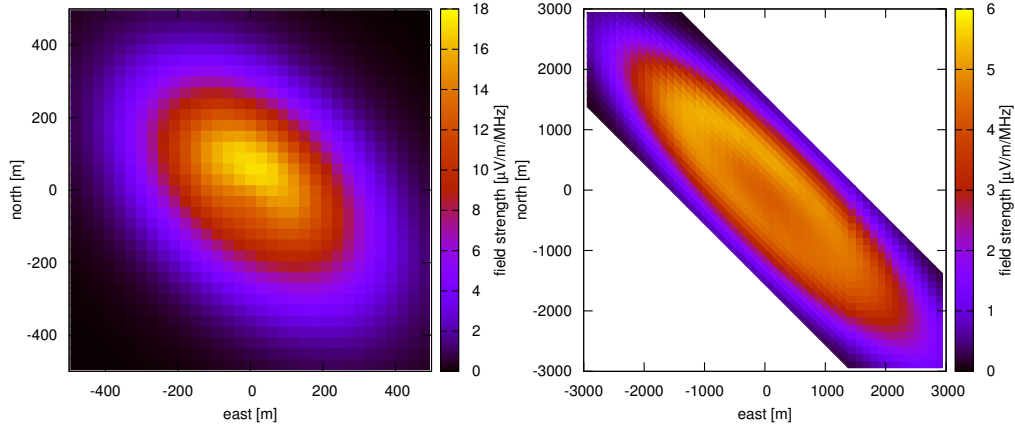


FIGURE 8. Simulated footprints of radio emission for an air shower with 50° (left) and 75° (right) zenith angles as predicted with CoREAS simulations [27].

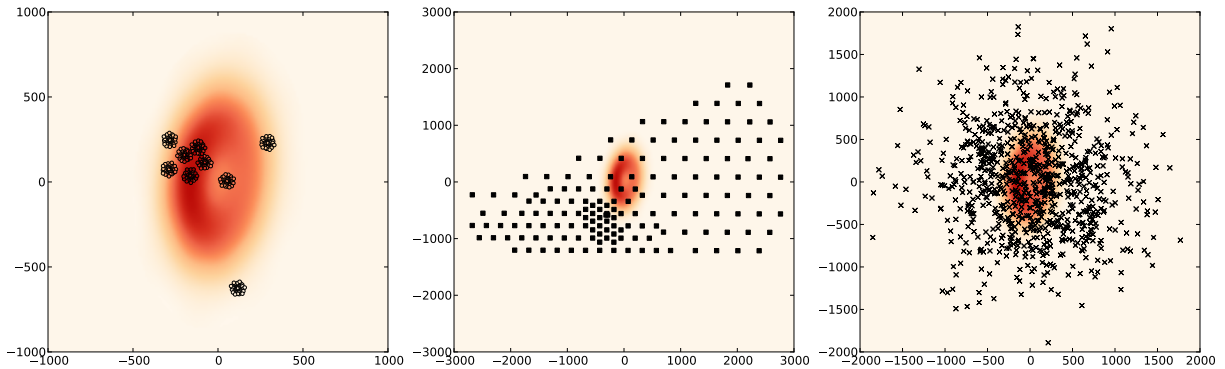


FIGURE 9. Antenna layouts for LOFAR (left), AERA (middle) and an SKA-like array (right). The axes denote distances in metres. The background colors represent the radio footprint of an air shower simulated with CoREAS. [26]

sensitivity in the radio signal diminishes for inclined air showers, coincident detection with radio antennas and particle detectors can yield valuable composition information via the ratio of the electromagnetic and muonic components in the air shower.

The second path being followed is that of very dense arrays such as LOFAR, which already today allows precise measurements of individual air showers. A new level in precision studies of air showers will be reached with the Square Kilometre Array (SKA) which is going to be available as of 2020 [26]. The SKA will have a significantly larger area than LOFAR covered with a much more uniform array of antennas (Fig. 9), also spanning a larger bandwidth of 50–350 MHz. With these advantages, the SKA will be a precision instrument for cosmic ray studies that can be used to study the transition from Galactic to extragalactic cosmic rays, particle physics at energies beyond the reach of the LHC and possible connections between lightning initiation and cosmic rays.

CONCLUSIONS

The radio detection technique has matured within the previous decade. We understand the radio emission physics and have developed analysis strategies to extract the particle arrival direction, energy, and mass composition information. In the next few years, these will be evaluated precisely in direct comparison with established particle, fluorescence light and Cherenkov light detectors. The radio measurements will also provide benefits to the existing detectors, in particular a precise and independent cross-check of the absolute energy scale. Further strong potential for the radio technique exists in the large-scale application for inclined air showers and in precision studies with dense arrays such as LOFAR and the future SKA.

REFERENCES

1. H. Falcke, W. D. Apel, A. F. Badea, et al., *Nature* **435**, 313–316 (2005).
2. D. Ardouin, A. Bellétoile, D. Charrier, et al., *Nucl. Instr. Meth. A* **555**, 148–163 (2005).
3. T. Huege, M. Ludwig, and C. W. James, *AIP Conf. Proc.* **1535**, 128–132 (2013).
4. J. Alvarez-Muñiz, W. Carvalho Jr., and E. Zas, *Astropart. Phys.* **35**, 325 – 341 (2012).
5. V. Marin, and B. Revenu, *Astropart. Phys.* **35**, 733–741 (2012).
6. K. D. de Vries, A. M. van den Berg, O. Scholten, and K. Werner, *Astropart. Phys.* **34**, 267 (2010).
7. K. Werner, K. D. de Vries, and O. Scholten, *Astropart. Phys.* **37**, 5–16 (2012).
8. F. D. Kahn, and I. Lerche, “Radiation from cosmic ray air showers,” in *Proc. Roy. Soc.*, 1966, vol. A-289, p. 206.
9. G. A. Askaryan, *Soviet Phys. JETP* **14**, 441 (1962).
10. R. Smida, F. Werner, R. Engel, et al., *Phys Rev. Lett.* in press (2014), arXiv:1410.8291.
11. H. Schoorlemmer, *Tuning in on cosmic rays*, Ph.D. thesis, Radboud Universiteit Nijmegen (2012).
12. H. R. Allan, *Prog. in Element. part. and Cos. Ray Phys.* **Vol. 10**, 171–302 (1971).
13. V. Marin, and the CODALEMA Collaboration, *Proc. 32nd ICRC, Beijing, China* **1**, 291 (2011).
14. F. Schroeder, and the Pierre Auger Collaboration, *Proc. 33rd ICRC, Rio de Janeiro, Brazil*, id 899 (2013).
15. A. Nelles, et al., *Proc. 33rd ICRC, Rio de Janeiro, Brazil*, id 558 (2013).
16. A. Aab, P. Buchholz, N. Förster, et al., *Phys Rev. D* **89**, 052002 (2014).
17. P. Schellart, S. Buitink, A. Corstanje, et al., *JCAP* **10**, 14 (2014).
18. T. Huege, R. Ulrich, and R. Engel, *Astropart. Phys.* **30**, 96–104 (2008).
19. W. D. Apel, J. C. Arteaga-Velazquez, L. Bähren, et al., *Phys. Rev. D* **90**, 062001 (2014).
20. F. Schröder, N. Budnev, O. Gress, et al., *Proc. 33rd ICRC, Rio de Janeiro, Brazil* id 452 (2013).
21. W. D. Apel, J. C. Arteaga, L. Bähren, et al., *Phys Rev. D* **85**, 071101(R) (2012).
22. S. Buitink, A. Corstanje, J. E. Enriquez, et al., *Phys. Rev. D* **90**, 082003 (2014).
23. A. Corstanje, P. Schellart, A. Nelles, et al., *Astropart. Phys.* **61**, 22–31 (2015).
24. W. Apel, J. Arteaga-Velázquez, L. Bähren, et al., *JCAP* **09**, 25 (2014).
25. T. Gousset, O. Ravel, and C. Roy, *Astropart. Phys.* **22**, 103–107 (2004).
26. T. Huege, J. D. Bray, S. Buitink, et al., *SKA science book* (2014), arXiv:1408.5288.
27. T. Huege, and C. W. James, *Proc. 33rd ICRC, Rio de Janeiro, Brazil* id 548 (2013).